A Chart for the Calculation of Radiative Temperature Changes

A Chart for the Calculation of Radiative Temperature Changes

by Giichi YAMAMOTO and Gaishi ONISHI

Geophysical Institute, Faculty of Science, Tôhoku University

(Received February 18, 1953)

1. Introduction

Besides the study of the radiation chart which is to calculate the radiative flux at any level in the atmosphere, there have been several investigations to calculate directly the temperature change due to radiation, *i.e.*, the divergence of the radiative flux. Recently COWLING [4] has discussed the possibilities of constructing such charts, but actually he did not show any such chart of practical use. Indeed, if we try to construct any chart according to COWLING's plans, we will encounter some practial incovenience which will oblige us to give up constructing the chart. For instance, in the flux divergence chart using the derivative of the transmission function, the numerical value of it becomes so large when the amount of absorbing medium is small that the chart will be inconveniently large in size. Thus, D. L. BROOKS [1] and BRUINENBERG [2] would have chosen to employ numerical tables instead of charts to calculate the flux divergence.

In the present investigation we will show one way of removing such practical difficulty and show the flux divergence chart which will be of practical use.

2. Theoretical Basis

Upward and downward fluxes U and D at height z are given by

$$U = \int_0^\infty B_\nu(T_z)\, d\nu + \int_0^\infty \int_{T_z}^{T_0} \frac{dB}{dT}\, \tau(u_z - u_s)\, dT\, d\nu, \tag{1}$$

$$D = \int_0^\infty B_\nu(T_z)\, d\nu - \int_0^\infty B_\nu(T_\infty)\, \tau(u_\infty - u_z)\, d\nu - \int_0^\infty \int_{T_\infty}^{T_z} \frac{dB}{dT}\, \tau(u_s - u_z)\, dT\, d\nu, \tag{2}$$

where

$$\int_0^\infty B_\nu(T_s) d\nu = B(T_s) = \sigma T_s^4, \tag{3}$$

T_s being the temperature at any height s, σ the STEFAN's constant, τ the transmission function of a slab, and u_s the amount of an absorber at height s, which is given by

$$u_s = \int_0^s \rho_s ds, \tag{4}$$

where ρ_s is the density of the absorber.

The rate of temperature change at height z is then given by

$$\frac{\partial T}{\partial t} = -\frac{1}{(\rho_{air})_z c_p} \frac{\partial}{\partial z}(U - D)$$

$$= \frac{-\rho_z}{(\rho_{air})_z c_p} \int_0^\infty \left\{ -B_\nu(T_\infty) \frac{d\tau(u_\infty - u_z)}{d(u_\infty - u_z)} - \int_{T_\infty}^{T_z} \frac{dB_\nu(T)}{dT} \frac{d\tau(u_s - u_z)}{d(u_s - u_z)} dT + \int_{T_z}^{T_0} \frac{dB_\nu(T)}{dT} \frac{d\tau(u_z - u_s)}{d(u_z - u_s)} dT \right\} d\nu, \tag{5}$$

where ρ_{air} is the air density. The first term in the brackets represents the escape of radiation to outer space. In the second and the third terms the numerical value of $\frac{d\tau}{du}$ is extremely large for a small value of u and this represents the fact that most of the radiation absorbed at a given level comes from the immediate vicinity.

COWLING [4] discusses the way of constructing charts and points out some of the difficulties. The main difficulty is that any variable, however to be defined, varies too greatly in the atmosphere. No chart can afford enough space to contain such a variable. BRUINENBERG [2] firstly established numerical method by replacing (5) as follows :

$$\frac{\partial T}{\partial t}=\frac{\rho_z}{(\rho_{air})_z c_p}\left[S'(u,T)+\int_T \frac{\partial S'}{\partial T}dT\right], \quad (6)$$

where

$$-S'(u,T)=\int_0^\infty B_\nu(T)\frac{d\tau(u)}{du}\,d\nu .$$

He gave extensive tabulations of functions S' and $\frac{\partial S'}{\partial T}$ for main absorbing matters, water vapour and carbon dioxide. Recently D. L. BROOKS [1] investigated another numerical method by transforming (5),

$$\frac{\partial T}{\partial t}=\frac{-\rho_z}{(\rho_{air})_z c_p}\left\{B(T_z)\overline{\frac{d\tau}{du}}+\sum\overline{\frac{d\tau}{du}}\,\Delta B(T)\right\}, \quad (7)$$

where $\overline{\frac{d\tau}{du}}$ means the mean value of $\frac{d\tau}{du}$ at two adjacent layers. His method is very interesting and mostly practical one. But, strictly speaking, the mean value is somewhat different from the actual value of $\frac{d\tau}{du}$ of the layer in the case of our atmosphere where water vapour decreases rapidly with height. To avoid this difficulty the graphical method is more suitable. Another difficulty is that the value of $\frac{d\tau}{du}$ is less well known than that of τ and no small inaccuracy may be hidden in his table. The merit of BROOKS' method is that variables of him are T and u which are easy to obtain and troublesome calculations are unnecessary in using his table. On the other hand using BRUINENBERG's table, we must perform other calculations and the same can be said about charts of COWLING's ideas. In considering such circumstances, we will try to modify BROOKS' table into a chart.

The value of $\frac{d\tau}{du}$ is large for small amount of absorbing medium, and becomes very small for large amount of it. For instance the value of $\frac{d\tau}{du}$ is 544 for very small precipitable water and 0.002 for 10 cm of it. If square root of $\frac{d\tau}{du}$ is adopted, the variation of its numerical value with u will be decreased considerably. This is the basic idea of our chart.

If we introduce the mean value of $\frac{d\tau}{du}$ about ν, given by

$$\int_0^\infty \frac{dB_\nu(T)}{dT}\,\frac{d\tau(u)}{du}\,d\nu=\frac{dB(T)}{dT}\,\overline{\frac{d\tau(u)}{du}}, \quad (8)$$

then we have from (5),

$$-\frac{(\rho_{air})_z c_p}{\rho_z}\frac{\partial T}{\partial t}=-\int_0^\infty B_\nu(T_z)\frac{d\tau(u_z-u_z)}{d(u_z-u_z)}d\nu-\int_{B(T_z)}^{B(T_s)}\frac{d\tau(u_s-u_z)}{d(u_s-u_z)}dB+\int_{B(T_z)}^{B(T_0)}\frac{d\tau(u_z-u_s)}{d(u_z-u_s)}dB. \quad (9)$$

I II III

Now we put followingly

$$dB = k\,d\theta, \quad (k \text{ is a constant}),$$

$$\left\{\left|\frac{d\bar{\tau}(u)}{du}\right|\right\}^{\frac{1}{2}} = R(u, T),$$

then we have

$$\int_B \frac{d\bar{\tau}(u)}{du}\,dB = -\frac{k}{2}\int_\theta R^2\,d\theta.$$

In general, we can write

$$\int \frac{d\bar{\tau}(u)}{du}\,dB = -\frac{k}{2}\int_\theta \left\{\frac{R}{w(\theta)}\right\}^2 w^2(\theta)d\theta$$

$$= -\int \left\{\frac{R}{w(B)}\right\}^2 dS(B), \qquad (10)$$

where

$$S = \frac{k}{2}\int w^2(\theta)\,d\theta.$$

Accordingly we can put variables in the polar coodinates, $S(B)$ being the argument and $\frac{R}{w(B)}$ the radius, and above integral (10) is given by the area in the polar coordinate diagram.

3. Construction of the Flux Divergence Chart

In considering the temperature change of the troposphere, we consider only two principal absorbing medium, *i.e.*, water vapour and carbon dioxide, and neglect ozone. Further, to avoid superfluous complications, we assume with some thereby inevitable error that the absoption bands of each gas are not overlapping. Practially we assume that water vapour is transparent between 13 and 17 μ. Then instead of (9) we have

$$\frac{\partial T}{\partial t} = -\frac{1}{\rho_{air}c_p}\left[\rho_z(H_2O)\left\{-\int B_\nu(T_s)\frac{d\tau(u_s-u_z)}{d(u_s-u_z)}d\nu - \int_{B(T_s)}^{B(T_z)}\frac{d\bar{\tau}(u_s-u_z)}{d(u_s-u_z)}dB + \int_{B(T_z)}^{B(T_0)}\frac{d\bar{\tau}(u_z-u_s)}{d(u_z-u_s)}dB\right\}_{H_2O}\right.$$

$$\left. + \rho_z(CO_2)\left\{-\int B_\nu(T_s)\frac{d\tau(u_s-u_z)}{d(u_s-u_z)}d\nu - \int_{B(T_s)}^{B(T_z)}\frac{d\bar{\tau}(u_s-u_z)}{d(u_s-u_z)}dB + \int_{B(T_z)}^{B(T_0)}\frac{d\bar{\tau}(u_z-u_s)}{d(u_z-u_s)}dB\right\}_{CO_2}\right]. \qquad (11)$$

Here we can treat the effects of water and carbon dioxide separately and obtain the rate of temperature change by adding both effects.

Now the most important part of the problem is concerning the transmission function and its derivative. COWLING [3] has calculated numerically the reasonable transmission of a column and YAMAMOTO [9] has obtained the transmission function of a slab which is essentially derived from ELSASSER's [5] formula with correction to adapt COWLING's calculation for large water path. Recently GOODY [6] has proposed a statistical model of absorption band and obtained an analytical formula for transmission function of a column which agrees with the numerical calculation of COWLING. [3] But he gives no mention on the transmission function of a slab. So we will adopt in the present investigation the transmission curve for a slab of water vapour obtained by YAMAMOTO [9] and the absorption coefficient of water vapour compiled by YAMAMOTO [10]. We also adopt here the slab transmission of carbon dioxide used by YAMAMOTO [10] in constructing his radiation chart.

Recent measurements by TOWNES & MERRITT [8] enable us to estimate the pressure correction with some confidence. According to the result which affirms LORENTZ' classical theory, we assume that the pressure effect on the half-width is proportional to pressure. And by the usual procedure we assume that the corrected optical thickness is given by

$$u_z^* = \int_0^z \rho_s \frac{p_z}{p_0}\,ds, \qquad (12)$$

where p_0 is the standard pressure, 1000 mb. By the same meaning we replace ρ_z of (9) or (11) by ρ_z^* given by

$$\rho_z^*\left(=\frac{\partial u_z^*}{\partial z}\right) = \rho_z\frac{p_z}{p_0}. \qquad (13)$$

The obtained chart for water vapour is shown in fig. 1 in which the radius is $\left(\left|\frac{d\tau}{du}\right|\right)^{\frac{1}{2}}_{H_2O}$ and the argument $B/2$. The method of calculation of flux divergence using the chart is shown diagrammatically in fig. 2, in which areas I, II and III correspond to contributions of the respective terms in (9) (it should be noticed that $\frac{d\tau}{du}$ is negative). Here we assumed that I of (9) is transformed to

$$\int_0^{\infty} B_\nu(T_z)\frac{d\tau(u_\infty - u_z)}{d(u_\infty - u_z)}d\nu = \int_0^{T_\infty}\frac{d\tau(u_z - u_z)}{d(u_\infty - u_z)}\,dB.$$

Thus the bracket $\left\{\quad\right\}$ of (9) is given by the area (I+II+III) and the required temperature change of the layer due to water vapour is obtained by multiplying the water vapour density to it and further dividing $(\rho_{air})_z c_p$. Inspite of our contrivance to abridge the chart by using polar coordinates, when the vapour density of the layer is large, that is, in the layer near the ground, the value of $\left(\left|\frac{d\tau}{du}\right|\right)^{\frac{1}{2}}_{H_2O}$ diminishes rapidly to small quantity, so that the area enclosed by the curve is also small and the accuracy of the computation decreases accordingly. At such cases we use the chart shown in fig.3 in which $\left(\left|\frac{d\tau}{au}\right|\right)^{\frac{1}{2}}_{H_2O} e^{-aB}$ is taken as the radius and $\frac{1}{2a}\ e^{2aB}$ as the argument. Even with this modification the chart is still considerably large if fully described, so that the upper part of the chart is omitted in fig. 3. This is because the parts of the areas for small values of u may practically cancel each other in II and III.

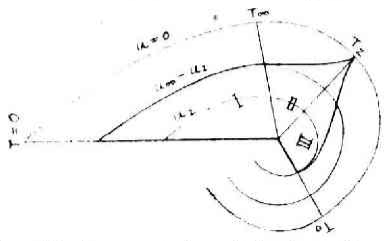

Fig. 2 Graphical computation of the flux divergence.

The flux divergence chart for carbon dioxide is shown in fig. 4. In this case we assumed that the absorption band of carbon dioxide is limmitted between 13-17μ. In this chart we took $\left(\left|\frac{d\tau}{du}\right|\right)^{\frac{1}{2}}_{CO_2}$ as the radius and $\frac{2B}{T^2}$ as the argument. The effect of carbon dioxide on the temperature change is practically small near the ground, so that the chart is to be employed mainly to calculate the temperature changes at the upper layer of the troposphere.

4. Comparison of Numerical Results Obtained by Various Methods

We will now calculate the rate of temperature change for a given atmospheric conditions by various methods and compare the results. For the purpose we will employ the atmospheric conditions used by D. L. BROOKS [1], that is, the result of the mean sounding for July, 1941 at Portland, Maine, U. S. A., and compute the temperature change at 902 mb level. For the sake of comparison the effective length of water vapour was taken to be

$$u^{**} = \int_0^z \rho_z \left(\frac{p_z}{p_0}\right)^{\frac{1}{2}} dz, \qquad (14)$$

which was adopted by BROOKS. The result of computation by assuming the clear sky is as shown in table 1.

Table 1

Rates of temperature change for atmospheric conditions used by BROOKS. (°C/day)

By use of BROOKS' tables	-2.25	
By due of BRUINENBERG's tables (due to BROOKS)	-1.7	
By use of ELSASSER's chart (due to BROOKS) (Mean temprature change between 957 and 851 mb)	-1.9	
By use of YAMAMOTO's chart (mean femperature change between 957 and 851 mb)	-2.16	-2.08
By use of the present chart	-1.90	-1.80

From the table we can see that BROOKS' value is largest and BRUINENBERG's smallest. Other values being between them. In the last column of table 1 were shown values of temperature change calculated by use of YAMAMOTO's chart and the present chart using the effective optical thickness given by (12). It will be seen that the values of temperature change decrease slightly compared with the respective values of the preceeding column.

Next, using LONDON's [7] model atmospher for March, north hemisphere, 0-10°, clear sky, the same comparison is given in table 2. Here, in the cases of BROOKS' method and Elsasser's chart, the optical thickness was assumed to be given by (14) and in other cases it was assumed to be given by (12). It will also be seen that the values of temperature change obtained by use of BROOKS' method are generally larger than those obtained by other methods, and that those obtained by ELSASSER's method are generally smallest. The contributions of water vapour and carbon dioxide were separately computed by use of the present chart. Generally the contribution of carbon dioxide is far smaller than that of water vapour. It is, however, interesting to note that the contribution of carbon dioxide near 14 km is rather heating of the layer.

Table 2

Rates of temperature change (°C/day) for LONDON's model atmosphere, 0–10°N, clear skies.

Height	By BROOKS' chart	By ELSASSER's chart	By YAMAMOTO's chart	By present chart		
				H_2O	CO_2	sum
0	-3.50					
		-1.26	-1.78	-2.20	-0.20	-2.40
1	-1.77	-1.36	-1.98	-1.73	-0.18	-1.91
2	-2.07	-1.42	-2.20	-1.64	-0.18	-1.82
4	-2.34	-1.66	-2.28	-1.87	-0.15	-2.02
6	-2.70			-2.29	-0.22	-2.51
		-1.86	-2.28			
8	-2.97	-1.86	-2.24	-2.29	-0.32	-2.61
10	-3.32	-1.92	-2.02	-2.29	-0.20	-2.49
12	-1.63	-2.00	-1.25	-1.74	0.00	-1.74
14	-0.61	-1.55	-0.67	-0.68	0.03	-0.65
16	-0.16			-0.14	-0.02	-0.16

References

1. BROOKS, D. L., : A Tabular me hod for fhe Computation of Temperature change by Infra Red Radiaton in the free Atmosphere. *J. Met.* 5, 313, 1950.
2. BRUINENBERG, A. : Een Numerieke Methode voor de Bepaling van Temperatuurs-Veranderingen door Straling in de vrije Atmosfeef. *Med. en verh. Ned. Met. Inst.* B, I, NO. 1, 1946.
3. COWLING, T. G. : Atmospheric Absorption on Heat Radiation by Water Vapour. *Phil. Mag.* 41, 109, 1950.
4. COWLING, T. G. : The Calculation of Radiative Temperature Chenges. *Cent. Proc. R. Met Soc.* 19. 1950.
5. ELSASSER, W. M. : Heat Transfer by Infra-Red Radiaetion in the Atmosphere. *Harvard Meteor. Stud.* No. 6. 1942.
6. GOODY, R. M. : A Statistical Model for Water-Vapour Absorption. *Quart. J. R. Met. Soc.* 78, 165, 1952.
7. LONDON, J. : The Distribution of Radiational Temperature Change in the North Hemisphere during March. *J. Met.* 9, 145, 1952.
8. TOWNES, C. H. & MERRITT, F. R. : Water Spectrum near One Centimeter Wave-Length. *Phys. Rev.* 70, 550, 1946.
9. YAMAMOTO, G. : On the Relation between Transmission Function of Column and that of Slab for Infra Red Absorption Band. *Sci. Rep. Tohoku Univ.* Ser. 5, 3. 130. 1951
10. YAMAMOTO, G. : On a Radiation Chart. *ibid.* 4, 9, 1952.

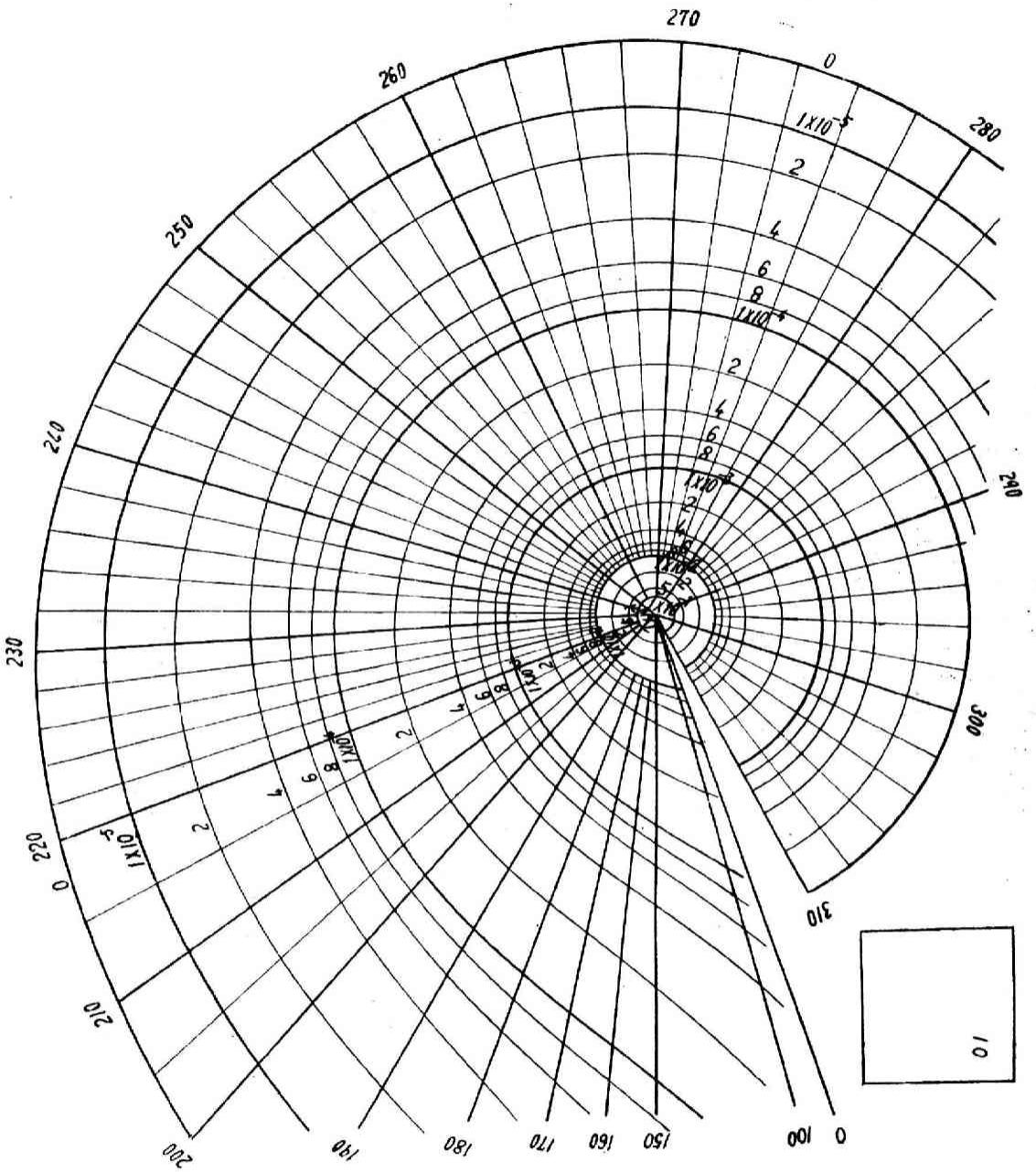

Fig. 1 Flux divergence chart of water vapour.

Radial lines express isotherms and circular lines constant-w_{H_2O} lines.

Unit of area : 10 cal. cm^{-2}. min^{-1}. per cm. of precipitable water.

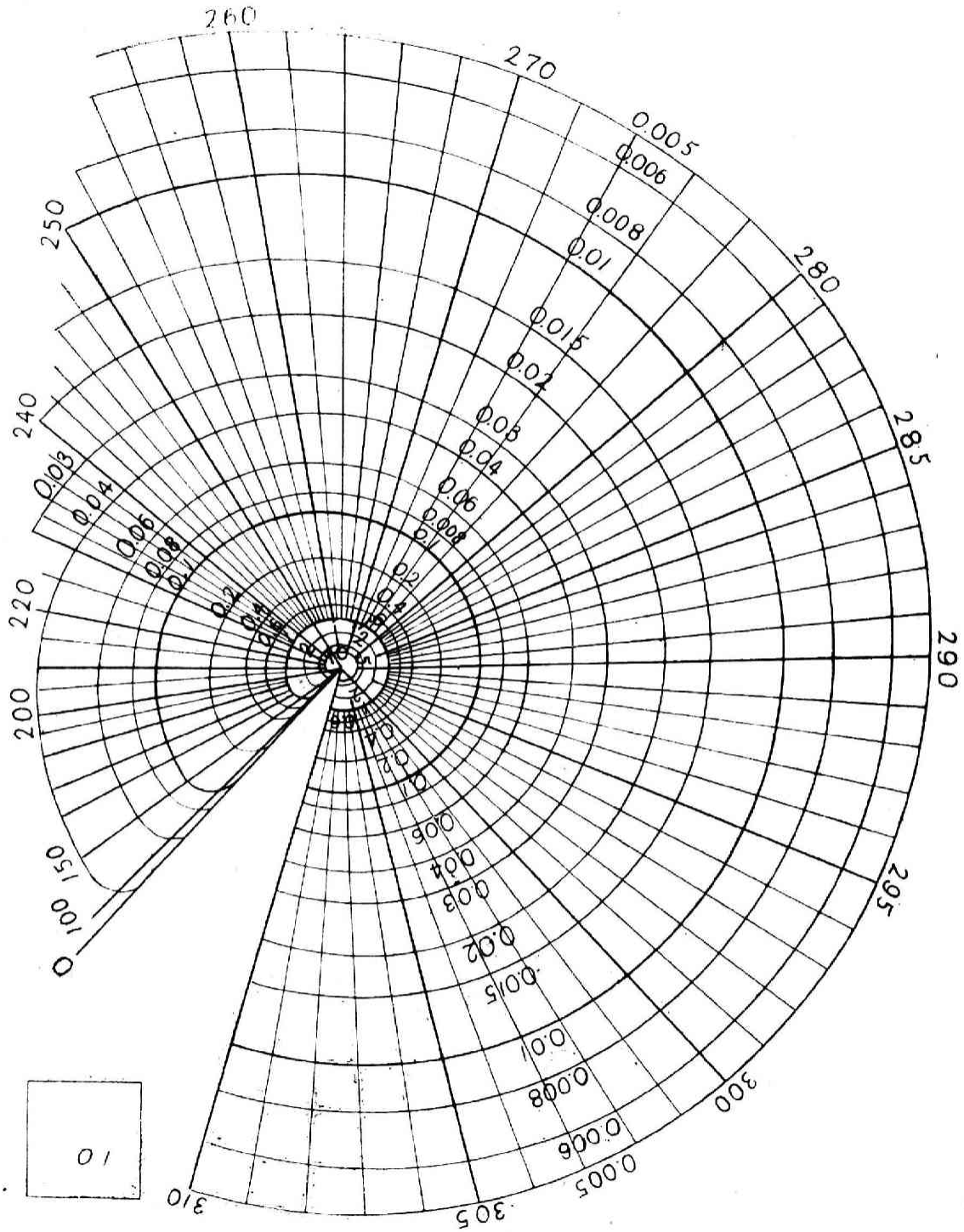

Fig. 3. Flux divergence chart of water vapour for use in lower atmosphere.
Radial lines express isotherms and circular lines express constant-w_{H_2O} lines.
Unit of area : 0.1 cal. cm^{-3}. min^{-1}. per cm. of precipitable water.

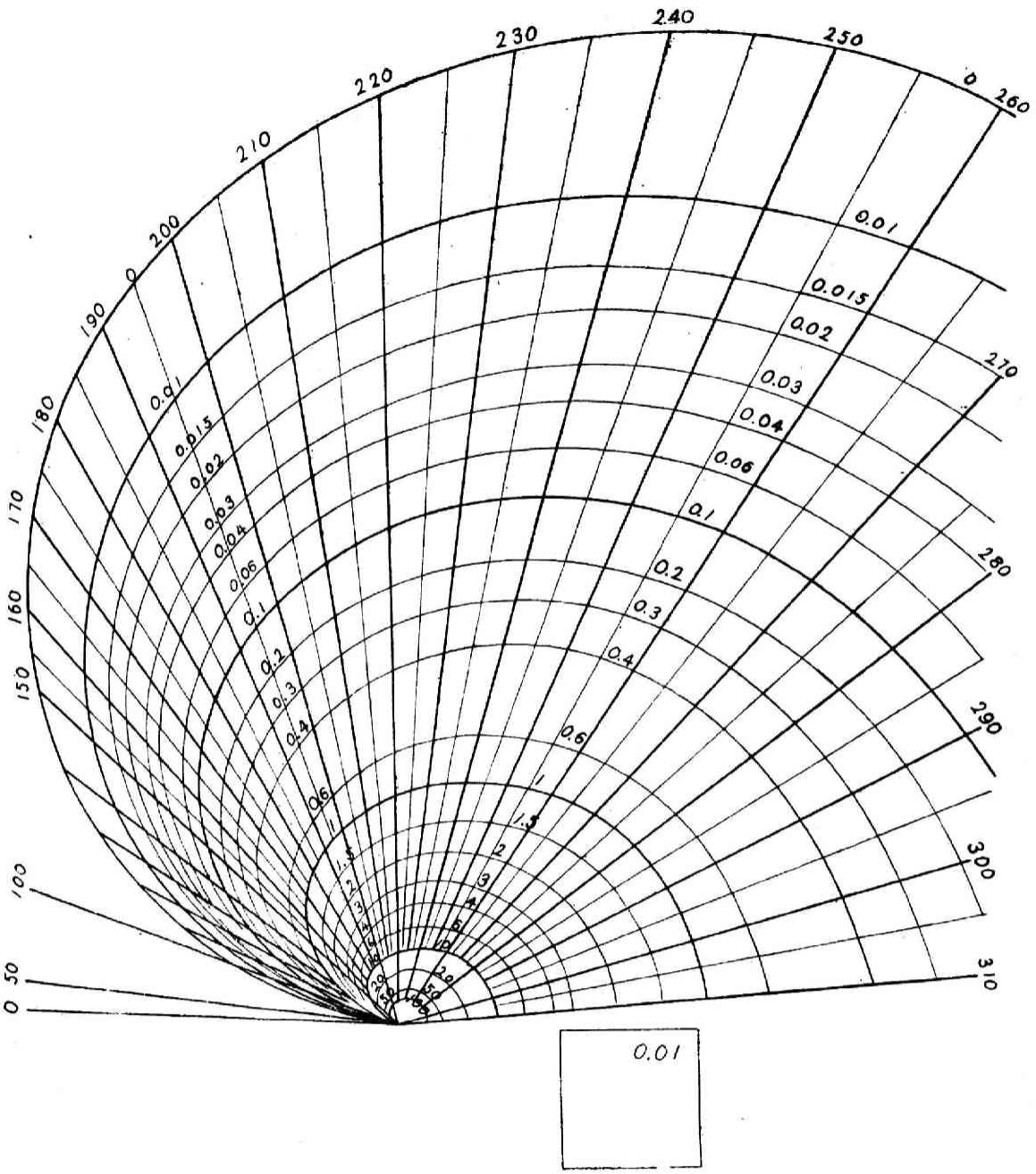

Fig. 4 Flux divergence chart of carbon dioxide.

Radial lines express isotherms and circular lines express constant-$u_{(CO_2)}$ lines.

Unit of area ; 0.01 cal· cm^{-2}. min^{-1}. per cm. of CO_2 in N. T. P.